Appl Microbiol Biotechnol (2014) 98:3529–3538
DOI 10.1007/s00253-013-5485-6

Self-assembly of virus-like particles of canine parvovirus capsid protein expressed from *Escherichia coli* and application as virus-like particle vaccine

Jin Xu · Hui-Chen Guo · Yan-Quan Wei · Hu Dong · Shi-Chong Han · Da Ao · De-Hui Sun · Hai-Ming Wang · Sui-Zhong Cao · Shi-Qi Sun

Received: 30 September 2013 / Revised: 18 December 2013 / Accepted: 20 December 2013 / Published online: 12 January 2014

Abstract Canine parvovirus disease is an acute infectious disease caused by canine parvovirus (CPV). Current commercial vaccines are mainly attenuated and inactivated; as such, problems concerning safety may occur. To resolve this problem, researchers developed virus-like particles (VLPs) as biological nanoparticles resembling natural virions and showing high bio-safety. This property allows the use of VLPs for vaccine development and mechanism studies of viral infections. Tissue-specific drug delivery also employs VLPs as biological nanomaterials. Therefore, VLPs derived from CPV have a great potential in medicine and diagnostics. In this study, small ubiquitin-like modifier (SUMO) fusion motif was utilized to express a whole, naturalVP2 protein of CPV in *Escherichia coli.* After the cleavage of the fusion motif, the CPV VP2 protein has self-assembled into VLPs. The VLPs had a size and shape that resembled the authentic virus capsid. However, the self-assembly efficiency of VLPs can be affected by different pH levels and ionic strengths. The mice vaccinated subcutaneously with CPV VLPs and CPV-specific immune responses were compared with those immunized with the natural virus. This result showed that VLPs can effectively induce anti-CPV specific antibody and lymphocyte proliferation as a whole virus. This result further suggested that the antigen epitope of CPV was correctly present on VLPs, thereby showing the potential application of a VLP-based CPV vaccine.

Keywords Canine parvovirus · Prokaryotic expression · Virus-like particles · Immunogenicity · Capsid protein

Introduction

Canine parvovirus (CPV) disease is an acute, highly contagious viral disease which can cause hemorrhagic gastroenteritis in adult dogs and myocarditis in puppies. CPV disease can induce high mortality and mobility; as such, CPVoutbreak can result in severe economic losses in dogs (Parrish 1990).For these reasons, this disease should be controlled by administering regular vaccination. Although conventional attenuated CPV vaccine has been extremely successful in reducing the number of disease outbreaks, the use of CPV in vaccination has raised several concerns and limitations. Among these limitations, such as attenuated virus strain could develop the mutation or virulence return under the selective pressure or impact of maternal antibody, mutation and virulence are enhanced, thereby causing CPV (Mohan et al. 2010). In addition, inactivated CPV vaccine can raise safety issues because of a possible virus spread during vaccine production and insufficient chemical inactivation of virus. Hence, new generation vaccines should be developed.

Virus-like particles (VLPs) have been recognized as safe and effective vaccine candidates for viral diseases. VLPs are virus-sized particles composed of rod-like or icosahedron supra-molecular structures (Johnson and Chiu 2000). These

J. Xu and H.–C. Guo contributed equally to this work and should be considered co-first authors

Electronic supplementary material The online version of this article (doi:10.1007/s00253-013-5485-6) contains supplementary material, which is available to authorized users.

J. Xu · H.-C. Guo · Y.-Q. Wei · H. Dong · S.-C. Han · D. Ao · D.-H. Sun · H.-M. Wang · S.-Q. Sun (✉)
State Key Laboratory of Veterinary Etiological Biology and National Foot and Mouth Disease Reference Laboratory, Lanzhou Veterinary Research Institute, Chinese Academy of Agricultural Sciences, Xujiaping 1, Lanzhou, Gansu 730046, China
e-mail: sunshiqi@caas.cn

J. Xu · D. Ao · S.-Z. Cao
College of Veterinary Medicine, Sichuan Agricultural University, Ya'an 625014, China

particles are also composed of multiple copies of one or more recombinant viral structural proteins, which are spontaneously assembled in particles without incorporating the viral genome. VLPs display antigens in orderly and repetitively, thereby inducing rapid, robust humoral immune responses and efficient T-cell responses (Grgacic and Anderson 2006). In addition, VLPs can package nucleic acid or other small molecules; VLPs can also be used as a delivery vehicle of a gene or a drug (Chang et al. 2011; Kitai et al. 2011). With in-depth research on the biological characteristics of viruses and recent technological advancement, VLP technology can be applied in the biological medicine field. Many kinds of genes encoding viral capsid proteins in *eukaryotic* expression systems and a few genes encoding viral capsid proteins in *prokaryotic* expression systems can effectively result in self-assembly; some of these viruses include hepatitis B virus (Mihailova et al. 2006), human papilloma virus (Ionescu et al. 2006), HIV gag proteins (Pillay et al. 2009), and porcine parvovirus (Sedlik et al. 1995). The expression of heterologous genes in *bacteria* is one of the simplest and most inexpensive methods used for research or commercial purposes compared with genes in *eukaryotic* expression systems, such as insect and mammalian cells. Many gene-fusion systems, including NusA, maltose binding protein (MBP), glutathione-*S*-transferase (GST), ubiquitin (UB), and thioredoxin (Trx) have been used to promote protein expression and purification (Guo et al. 2013). Small ubiquitin-like modifier (SUMO) protein, a ubiquitin-related protein, has also been developed as an effective biotechnological tool because SUMO usually promotes the correct folding and the structural stability of fusion proteins; as a result, the functional production of partner proteins is enhanced compared with an untagged version (Malakhov et al. 2004).

The virion of CPV is a non-enveloped, icosahedral particle with a diameter of 26 nm (Tsao et al. 1991). The genome of CPV is a single-stranded negative-sense DNA molecule of approximately 5.2 kb with two promoters that induce the expression of three structural viral proteins (VP1,VP2, and VP3) and two non-structural proteins (NS1 and NS2) by alternately splicing the viral mRNAs.VP2 (64 kDa), an NH_2-terminally truncated form of VP1 (84 kDa), is the major component of the capsid of a virion.VP3 is derived from VP2 via post-translational proteolytic cleavage; VP3 is present only in natural virions (Gallo Calderon et al. 2012; Parrish et al. 1991).As the main subunit component of CPV capsid,VP2 protein exhibits good immunogenicity; many antigen epitopes are mainly present in VP2 protein (Singh et al. 2006). In addition, VP2 protein expressed in vitro can self-assemble into VLPs (Yuan and Parrish 2001). VP2 protein is also considered as one of the important candidates of CPV vaccine (Dahiya et al. 2012; Patial et al. 2007).

In this study, a SUMO fusion protein system in *E. coli* was developed. Water-soluble CPV VP2 proteins were also produced. After the SUMO moiety was removed from the fusion proteins, the VP2 proteins can be assembled to form VLPs with a size and shape resembling a natural CPV. We also determined whether or not different factors, including pH, ionic strength, and temperature, can affect the efficiency and quantity of the assembly. The immune response of mice vaccinated with the CPV VLPs suggested that VLPs can correctly present the antigen epitope of a CPV capsid to immune cells. VLPs can be a used as a vaccine candidate for the CPV control program.

Materials and methods

Cells

Feline kidney F81 cells were cultured at 37 °C in 5 % CO_2 atmosphere in Dulbecco's modified Eagle's medium (DMEM, Gibco). DMEM was supplemented with 10 % fetal bovine serum (FBS; Gibco) containing 100 units/ml penicillin G sodium (BBI) and 100 μg/ml streptomycin sulfate (BBI).

Virus isolation and titration

Virus isolated by minor revision as described previously (Ntafis et al. 2011). Faecal and tissue samples were homogenized (10 %, w/v) in D-MEM and centrifuged at 8,000×*g* for 10 min. Supernatants were treated with antibiotics (1,000 IU/ml penicillin and 100 mg/ml *streptomycin*) for 30 min, inoculated on partially confluent F81 cell cultures and then, they were incubated at 37°C in a 5 % CO_2 incubator. After an adsorption period of 1 h, DMEM was added. Cells were daily observed for cytopathic effect (CPE) for 5 days. Viruses were propagated in cells and cultured for three blind passages. The genetic analysis of isolated virus was performed as our previous report (Xu et al. 2013). The virus belongs to genotype CPV-2a and genome of virus was uploaded to GenBank (ID: JQ268283.1, http://www.ncbi.nlm.nih.gov/nuccore/390098350) (Xu et al. 2013). CPV was purified by ultracentrifugation in sucrose gradient. In brief, cells infected with CPV were frozen and thaw for three times, and then centrifuged at 4,000 rev/min for 30 min. The supernatant was further centrifuged at 10,000 rev/min for 30 min and mixed with 8 % PEG6000 and 3 % NaCl at 4°C overnight. The mixture was centrifuged at 10,000 rev/min for 60 min. The pellet was dispersed in phosphate buffered saline (PBS) and added in sucrose gradient (20–65 %), which was centrifuged at 15,0000×*g*/min for 3 h after stay at 4°C overnight. Sucrose gradient was extracted every 0.5 ml as 1 unit. Virus in each unit was detected by quantitative PCR. This virus strain had been deposited in China General Microbiological Culture Collection Center (CGMCC; accession number: 7983).

The supernatants of F81 cells infected with CPV-2a were monitored for virus titers by tissue culture infectious dose 50 ($TCID_{50}$). In brief, supernatant was diluted 10-fold multiple proportions with DMEM, and added 0.1 ml into each well of 96-well plate (Nunc, Roskilde, Denmark), each dilution repeat eight wells, positive and negative controls were set with Chinese reference strain CPV-CD (GeneBank: JF681986.1, kindly supplied by Dr. Peng, Sichuan Agricultural University, China) and DMEM medium, respectively. F81 cells at a density of 1,000 cells/well were spontaneously seeded into the same wells (0.2 ml/wells totally).The plate was incubated at incubator with 37°C, 5 % CO_2. After 72 h, the cells were washed with PBS for two times and fixed with 4 % paraformaldehyde (Aldrich, Steinheim, Germany) for 10 min in room temperature, and then permeabilized with 0.5 % Triton X-100.Subsequently, the cells were stained with mouse anti-CPV monoclonal antibody (Sigma, Shanghai, China) for overnight at 4°C, and stained with FITC-conjugated anti-mouse IgG. The plate was detected with the fluorescence microscope (Olympus, Japan), and the tissue culture infectious dose 50 ($TCID_{50}$) was calculated by Reed–Muench method.

Analysis of CPV VP2 structure

The homology model was constructed using Swiss-Model (Arnold et al. 2006), and the ribbon diagram was prepared using Swiss-PDB Viewer (Guex and Peitsch 1997).

Construction of VP2 expression plasmid

F81 cell pellets infected with *CPV-2a* were boiled for 10 min and immediately chilled in ice for 5 min to obtain a DNA template (Mohan et al. 2010). A pair of primers with *Bsm*BI and *Bam*HI sites was used (VP2 F: 5 -TGTCGTCTCAAGGT ATGAGTGATGGAGCAGTTC-3 , VP2 R: 5 -CGGGATCC GTTAATATAATTTTCTAGGTGCT-3) to amplify the VP2 gene. PCR amplification was performed using PrimeSTAR HS DNA polymerase kits (TaKaRa, China) in a Bio-Rad cycler (USA). The detailed procedure of PCR is as follows: denaturation at 98°C for 10 s; annealing at 50°C for 5 s; and polymerization at 72°C for 130 s with 35 cycles.PCR products were detected in 1 % agarose gel and visualized under UV light. The VP2 gene was then subcloned in a pSMK vector (Guo et al. 2013; Yin et al. 2010), and the final plasmid was labeled as pSMK-VP2. The constructed plasmid also comprised a 6× His tag and SUMO tag fused in the N terminus of VP2 to simplify protein purification. Recombinant plasmids were confirmed by endonuclease digestion and sequencing. These recombinant plasmids were then purified from *Escherichia coli* DH5α by using a plasmid midi kit (Qiagen). Purified products were used in the transformation.

Expression and purification of VP2 protein

The recombinant expression plasmids were transformed into *E. coli* BL21-codon Plus (DE3)-RIL competent cells (Stratagene) according to the manufacturer's protocol. A single colony of the transformant was grown in Luria–Bertani (LB) broth containing kanamycin (50 μg/ml) and chloramphenicol (34 μg/ml) at 37°C until the optical density (OD_{600}) reached 0.6. Isopropyl β-D-thiogalactoside (IPTG) was added to obtain a final concentration of 0.05 mM, and the cultures were incubated for 12 h at 16°C and 150 rev/min. Cells were harvested by centrifugation at 10,000 rev/min at 4°C for 30 min and resuspended in buffer A (500 mM NaCl, 20 mM Tris–HCl, 20 mM imidazole, 2 mM DTT, 0.05 % Triton X-100; pH=8.0). The cells were then lysed by sonication using pulses of 3 s with 3 s off during 6 min in an iced water bath. The cell lysate was centrifuged twice (12,000 rev/min) for 20 min each time. The supernatant were collected and stored at −80°C until use.

His-sumo-VP2 protein was purified by affinity chromatography under native conditions. The supernatant was transferred to a nickel affinity chromatography resin column pre-equilibrated with buffer A, incubated for 1 h at room temperature, and shaken gently to allow resin to combine with the target protein. The protein was washed with buffer A and then eluted with buffer B (500 mM NaCl, 20 mM Tris–HCl, 300 mM imidazole, 2 mM DTT, 0.05%Triton X-100; pH= 8.0) five to six times. The samples were analyzed by SDS-PAGE and Western blot.

SDS-PAGE and Western blot

The purified His-sumo-VP2 protein was subjected to 8 % SDS-PAGE and transferred to nitrocellulose (NC) membranes. Anti-His mouse primary antibody diluted in PBST (1:2,000) was used to detect VP2 fusion proteins in Western blots. The secondary antibodies were horseradish peroxidase (HRP)-conjugated goat anti-mouse IgG antibodies (1:6,000; Sigma). The protein bands were visualized using Amersham ECL Plus Western Blotting Detection Reagents (GE Healthcare).

Assembly and characterization of CPV VLPs

The purified His-sumo-VP2 protein and Sumo protease (ULP1) were placed in a dialysis bag at a ratio of 100:1 (vol/vol). Dialysis was conducted against buffer C (50 mM Tris–HCl buffer with NaCl at different concentrations and pH). His-sumo-VP2 protein was cleaved at 4°C for 15–16 h and continuously stirred. The liquid in the bag was further examined by transmission electron microscopy (TEM) and dynamic light scattering (DLS) to detect VLP assembly. The amounts of proteins purified were measured by a Micro BCA™ protein

assay kit (Pierce, Rockford, IL, USA) by measuring their UV absorbance at 562 nm.

Vaccination of mice with CPV VLPs

The mice received humane care in compliance with the guidelines of the Animal Research Ethics Board of Lanzhou Veterinary Research Institute, Chinese Academy of Agricultural Sciences (CAAS), China. *BALB/c* mice were purchased from the animal house of Lanzhou Veterinary Research Institute and raised in isolation cages.

Four-week-old male *Balb/C* mice were randomly divided into three groups, with six mice in each group. The mice in Group A were vaccinated with PBS as a blank control; the mice in Group B were vaccinated with CPV VLPs (20 μg protein/mice, pH 7.0, 150 mM NaCl); and the mice in Group C were vaccinated with CPV purified from F81 cells (20 μg protein/mice). At 14 days after the first immunization with subcutaneous injections, the second immunization was performed using the same method. Serum samples were collected from the tail at 7, 14, 21, and 28 days after immunization and used in serological tests.

ELISA for CPV specific antibody

CPV specific antibodies were detected using an indirect ELISA method. Briefly, 96-well microtiter plates (Nunc, USA) were coated with the monoclonal mouse antibody against CPV in 0.1 M carbonate/bicarbonate buffer (pH 9.6) and incubated overnight at 4°C. After three washes in PBST, the plates were blocked with 100 μl PBST containing 5 % non-fat dry milk for 1 h at 37°C. After three washes in PBST, diluted purified CPV in 1× PBS was added and incubated for 1 h at 37°C. Then mouse serum (1:100) with PBS containing 1 % non-fat dry milk was added, and plates were again incubated for 1 h at 37°C. After three washes in PBST, 100 μl diluted rabbit anti-mouse IgG peroxidase conjugate (Sigma, UK) in PBST containing 1 % non-fat dry milk at a 1:2,000 dilution was then added for 1 h at 37°C. The plates were then washed three times, and the colorimetric reaction was developed using 50 μl substrate solution (FAST *o*-phenylenediamine dihydrochloride; Sigma) for 15 min at 37°C. Color development was stopped with 50 μl of 2 N H_2SO_4, and OD was read at 490 nm.

Detection of neutralization antibody

The sera obtained from the mice were analyzed to determine the neutralizing antibody titers by using a micro-neutralization assay with a monolayer of F81 cells. Double dilutions of the sera were reacted with 100 $TCID_{50}$ of *CPV-2a* at 37°C for 1 h. The cells were then added as indicators of residual infectivity, and the microplates were incubated at 37°C for 3 days prior to fixing and staining. The endpoint titers were calculated as the reciprocal of the last serum dilution to neutralize 100 $TCID_{50}$ homologous *CPV-2a* in 50 % of the wells.

T-lymphocytes subpopulations assay

For flow cytometric analysis of splenocytes, 1×10^6 cells were washed in cold PBS containing 1 % albumin from bovine serum, centrifuged, and resuspended in cold PBS. The splenocytes were stained with rabbit anti-mouse CD3: Percp/CD4: APC/CD8: PE at the dilution recommended by the manufacturer (BD, USA). The cells were incubated for 30 min at 4°C and washed three times with cold PBS buffer. The samples were analyzed with FACScan (BD Biosciences).

T-lymphocyte proliferation assay

T-lymphocyte proliferation assay was performed using the Cell Titer $96AQ_{ueous}$ Non-Radioactive Cell Proliferation Assay (Promega, USA). Mouse spleens were removed under sterile conditions and ground through a sterile cuprous mesh (200 meshes) at 56 days after the first immunization. The spleen cells were immersed in RPMI 1640 medium with 10 % FBS, added to the lymphocyte separation medium (Sangon, China), homogenized, and centrifuged at 1,000 rev/min for 10 min. Pellets were discarded; buoyant cells were washed thrice in RPMI 1640 medium with 10 % FBS. The T-lymphocytes in 96-well plates (5×10^4 cells per well) were co-cultured with concanavilin A (ConA; final concentration of 10 μg/ml)in RPMI 1640 supplemented with 10 % FBS (Gibco, Life Technologies, Vienna, Austria), and maintained at 37°C in a humidified 5 % CO_2 atmosphere for 60 h. 3-(4,5-Dimethylthiazol-2-yl)-5-(3-carboxymethoxyphenyl)-2-(4-sulfophenyl)-2*H*-tetrazolium, inner salt (MTS) was added to each well and incubated for 4 h at 37°C in 5 % CO_2. The absorbance at 490 nm was determined. The results were expressed as a percentage of untreated control subjects.

Results

Topology of CPV VP2 protein

The CPV VP2 protein contains 584 amino acids. The physicochemical property of the VP2 protein was analyzed by using ExPASy proteomics server software online. The results showed that the molecular weight of VP2 is approximately 64.701 kDa, and the isoelectric point is 5.52. The instability index of VP2 is 29.52 and the average of hydropathicity is −0.498, indicating that the VP2 protein is stable and can aggregate. Figure 1 shows that VP2 contains three helixes; these helixes are located between 118 and 119, 123 and 131, and 246 and 249 amino acids, respectively. In addition, the

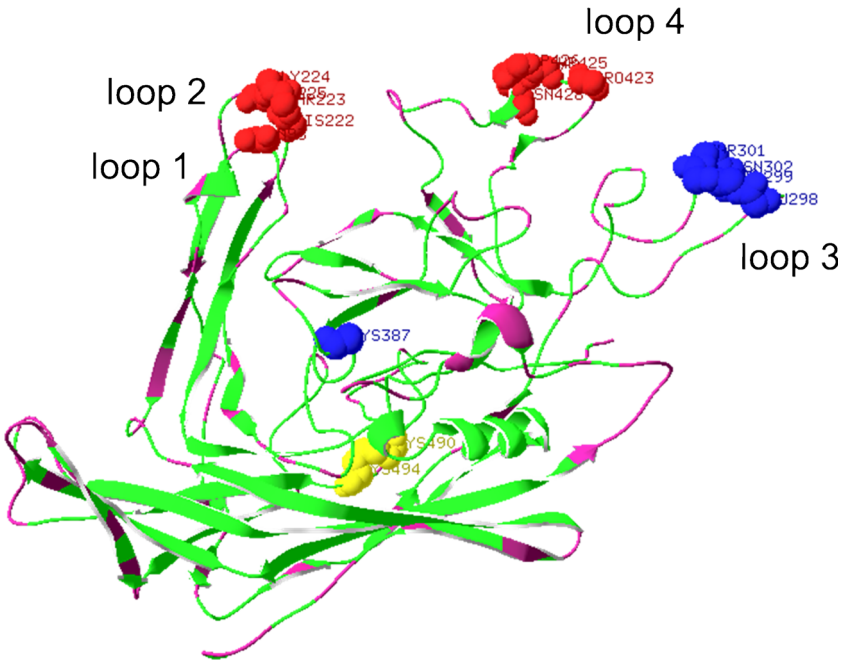

Fig. 1 Homology model of the capsid protein VP2 of CPV using the coordinates from the solved empty capsid viral protein (PDB: 2CAS). Antigenic residues implicated in antigenic sites are labeled and shown in spheres with different colors: A site, *red*; B site, *blue*. Accessible residues are shown in *magenta*. The only disulfide bond connecting *Cys*490 and *Cys*494 is highlighted by *yellow spheres*. The surface-exposed loops are labeled 1 to 4. The homology model is constructed using SWISS-MODEL, and the ribbon diagram is prepared by Swiss-PDB Viewer

only disulfide bond is located between Cys490 and Cys494 of VP2. Some antigenic sites are also found in VP2 proteins, and all of the amino acids in these sites are located at the very ends of loops 1, 2, and 4 in site A and at loop 3 in site B (Langeveld et al. 1993).

Expression and purification of the fusion VP2 protein

To obtain the soluble protein expressed in bacteria, we used Sumo tag in the recombinant plasmid. Figure 2 shows that His-sumo-VP2, or water-soluble SUMO fusion proteins, was strongly induced by IPTG. The expression efficiency was further improved at 16 °C with lower IPTG concentration and rotation speed than the conditions at 37°C for 3–4 h (data not shown). In addition, the yield of the purified protein produced by recombinant bacterial clone >20 mg/l of culture is significantly higher than the purified protein produced by the bacterial expression vector pET-28b (Park et al. 2007). The molecular mass of His-sumo-VP2 fusion protein is approximately 87 kDa. The recombinant protein is water-soluble; hence, this protein was used for further purification by Ni-NTA affinity chromatography under natural conditions. Although some unspecific bands with lower molecular weight were detected after elution (Fig. 2a) or digestion (Fig. 2b), a specific band of VP2 with a size of approximately 65 kDa was found on the NC membrane by using a specific anti-CPV primary antibody (Fig. 2c). The results suggested that a specific fusion protein with high quality was obtained.

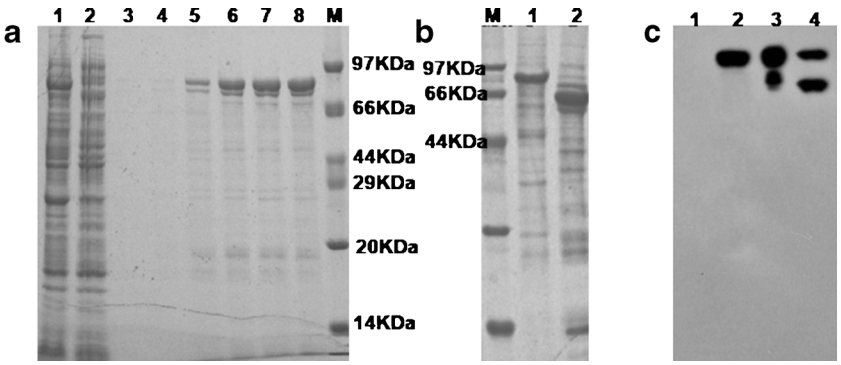

Fig. 2 Expression of CPV VP2 protein was analyzed by SDS-PAGE (**a** and **b**); Western blot analysis (**c**) using an anti-CPV polyclonal antibody. **a** *Lane 1*, cell lysate after induction of IPTG; *lane 2*, cell lysate before induction of IPTG; *lanes 3 to 4*, wash buffer; *lanes 5 to 8*, the first elution to the fourth elution. **b** *Lane 1*, purified His-sumo-VP2 protein; *lane 2*, His-sumo-VP2 protein digested by enzyme. **c** *Lane 1*, cell lysate before induction of IPTG; *lane 2*, cell lysate after induction of IPTG; *lane 3*, purified His-sumo-VP2 protein; *lane 4*, His-sumo-VP2 protein digested by enzyme. The molecular weight (*MW*) of His-sumo-VP2 protein is approximately 85 kDa. The VP2 protein is approximately 65 kDa

Assembly and characterization of VLPs

Extracts containing SUMO fusion proteins were purified on a Ni_2^+-resin and treated with SUMO protease to remove the His-Sumo moieties. The cleavage products contained VP2 soluble protein (with molecular weights of approximately 65 kDa) and His-Sumo tag (Fig. 2b), which was used as a starting material to assemble CPV VLPs. To determine the efficiency of VLP assembly under different conditions, we used NaCl and pH to adjust the condition in the dialysis buffer (Fig. S1).

Figure 3b shows that the size of VLPs under alkali condition (pH 8.0) is approximately 30 nm by DLS. However, VLPs easily aggregate with many particles of VP2 proteins as shown in the TEM image; such aggregation could be induced by incorrect protein packaging (Fig. 3d). The TEM image also shows that the CPV VLPs were uniform and few impurities were found under neutral conditions than under alkali conditions (Fig. 3c). This result is consistent with that of DLS, in which a great amount of VLPs exhibits the same dimensions of 25 nm as a wild virus under neutral conditions. In theory, the isoelectric point of VP2 protein is 5.5.We selected a slightly acidic condition (pH=6.5) to prevent the flocculating precipitation of CPV VP2 protein caused by low pH and to detect the efficiency of VLP assembly. Figure 3a shows that VLPs with the same dimension as CPV virions could be detected by DLS. However, the quantity of VLPs with approximately 25 nm was less than that under neutral conditions (pH 7.0).

Considering the nanometer particle size, we found that pellets with a dimension of approximately 20 to 30 nm could be determined according to the packing result of different NaCl concentrations but without the participation of NaCl. However, the quantity of pellets with a dimension of <20 nm increased to approximately 150 mM. The highest amount of pellets, with dimensions almost similar to those of the virus, was obtained at physiological conditions. Otherwise, the amount of pellets evidently reached equilibrium compared with the wave crest, and the size of pellets decreased as salt concentration increased.

An increase in ionic strength (NaCl) from 0 to 300 mM at pH 7.0 produced an increase in particle size as measured by DLS (Fig. 3b). Although VLPs with a diameter ranging from 20 to 30 nm can be detected without NaCl, smaller particles in DLS were more abundant than those under conditions exhibiting ionic strength. VLPs with a size of approximately 25 nm increased; smaller or larger VLPs decreased as ionic strength remained stable at 150 mM. As the concentration of NaCl increased to 300 mM, the peak of the curve increased on the coordinates in DLS, suggesting that the ratio of larger VLPs increased compared with that at 150 mM NaCl. However, the ratio of smaller and larger VLPs also increased compared with that at 150 mM NaCl. Hence, in our study, especially, in animal experiment, we selected the VLPs

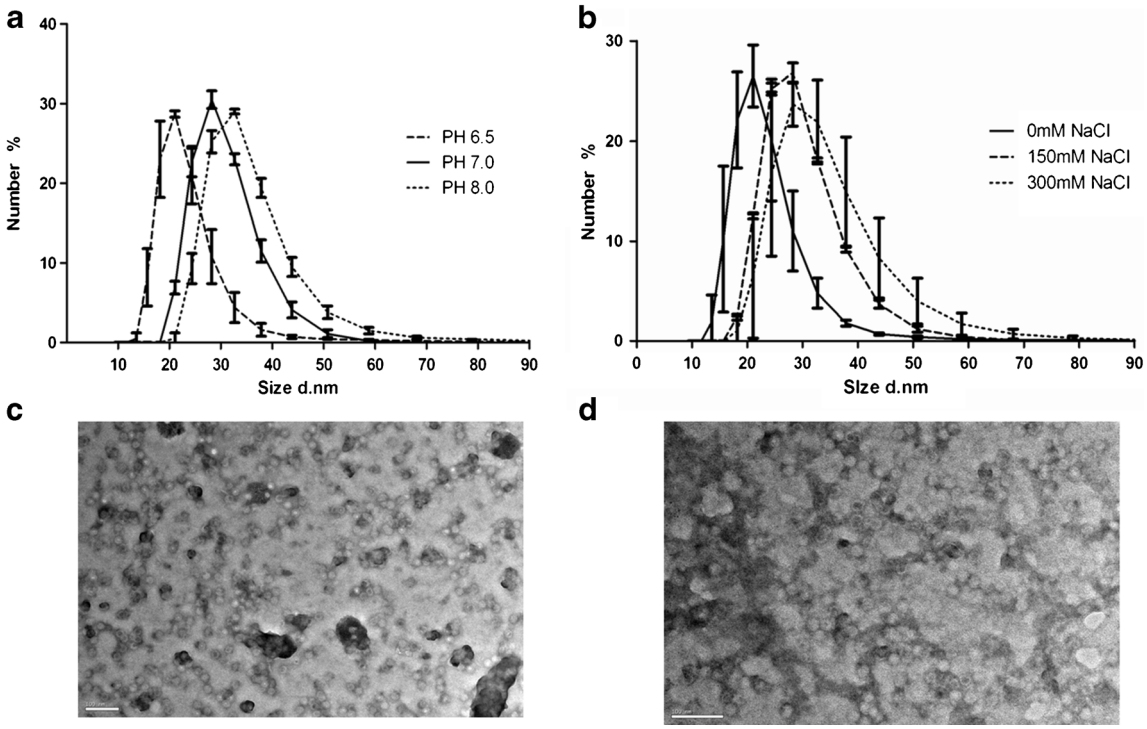

Fig. 3 **a** Percentage of CPV VLPs at different pH value (6.5, 7.0, 8.0). **b** Percentage of CPV VLPs at different NaCl concentrations (0,150, 200 mM). **c** TEM image of CPV VLPS in buffer with 150 mM NaCl (pH 7.0). **d** TEM images of CPV VLPs in buffer with150 mM NaCl (pH 8.0)

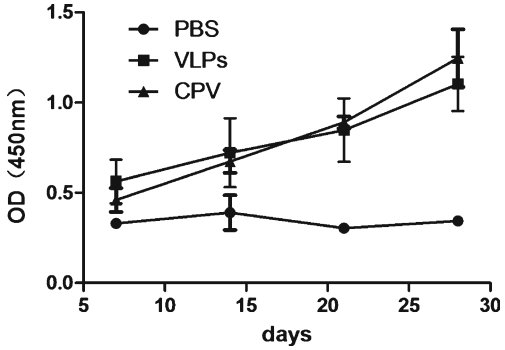

Fig. 4 CPV specific antibody titer of mice by indirect ELISA

assembled under the condition at pH 7.0 and 150 mM NaCl to inoculate the mice. This condition will ensure the assembly efficiency of VLPs is optimal.

Level of specific antibody in mice

To determine whether or not CPV VLPs can induce specific antibody response in mice, we immunized the mice with CPV VLPs subcutaneously; the two other groups of mice were immunized with CPV as the positive control and PBS as the negative control. Each mouse was bled at 7, 14, 21, and 28 dpi (days post inoculation) to determine the titers of specific antibodies. The results showed that the CPV-specific antibodies were efficiently induced by immunizing with CPV VLPs (Fig. 4).The antibody titer increased as time lapsed and further increased after a second vaccination was performed at 14 dpi. In addition, highly significant differences were observed between the mice inoculated with PBS and with either CPV VLPs or CPV ($p<0.01$). However, no significant difference was found between the mice inoculated with CPV VLPs and CPV ($p=0.9248$, $p>0.05$; Fig. 4).

Level of neutralizing antibody in mouse

Considering that the level of neutralizing antibodies mainly correlates with the protection of vaccinated animals against CPV infections, we assessed the anti-viral neutralizing serum antibody titers from immunized animals. High neutralizing antibody titers were induced in mice immunized with CPV VLPs; this result is similar to the high titers in the sera of the group immunized with whole CPV (Fig. 5). The neutralizing titers from animals in all of the vaccinated groups were significantly higher than those observed from the group immunized with PBS alone ($p<0.0001$). These results showed that no significant difference was found between the mice inoculated with CPV VLPs and whole CPV ($p=0.6746$; Fig. 5).

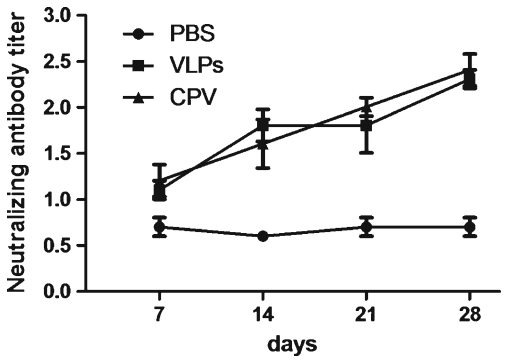

Fig. 5 Virus neutralizing antibody response to CPV after the mice were immunized by microtiter assay via F81 cells. Neutralizing antibody titers are presented as the mean from each group

T-lymphocyte subpopulation assay and lymphocyte proliferation test

VLPs can simultaneously induce specific humoral immune response and cellular immune response. To further confirm the immune efficiency of CPV VLPs in mice, we performed T-lymphocyte subpopulation assay and lymphocyte proliferation test by using mouse lymphocytes. For T-lymphocyte subpopulation assay, the mouse lymphocytes in the peripheral blood were collected at 56 dpi, and the proportions of CD4+ and CD8+ cells were determined by flow cytometry (Table 1). CD3+ cells were significantly upregulated in both groups immunized with CPV VLPs ($p<0.05$) or CPV ($p<0.05$) groups compared with the PBS group. The expressions of CD4+ cells and CD8+ cells were significantly increased in the mice immunized with CPV VLP or whole CPV virion.

For the lymphocyte proliferation test, the spleen lymphocytes of mice were aseptically collected at 56 days after immunization. Non-specific irritant Con A was used to stimulate responses; the mice were then vaccinated with the CPV VLPs or whole CPV and exhibited a highly specific T-cell response. The T-cells harvested from VLP-immunized animals and the cells harvested from CPV-immunized animals significantly proliferated compared with the unvaccinated mice, but the difference was not significant between the mice inoculated with CPV VLPs and whole CPV ($p=0.7773$; Fig. 6).

Discussion

Heterologous protein accumulation in *E. coli* often occurs in inclusion bodies. The process by which inclusion bodies are purified is complex, arduous, and time consuming. In addition, refolding of proteins in inclusion bodies can deactivate proteins. Although many strategies have been proposed to reduce these inclusion bodies or promote the solubility of heterologous proteins, heterologous protein expression by tag fusion is a potential development. Among these fusion tags, SUMO tag provides advantages compared with other fusion tag technologies, such as correct fusion protein folding, target protein protection from degradation, simple

Table 1 The subpopulations of PBMC in mice

	$CD3^+$ cells	$CD4^+$ cells	$CD4^+/CD3^+$ %	$CD8^+$ cells	$CD8^+/CD3^+$ %	$CD4^+/CD8^+$
CPV	3088±40	336±10	10.9±0.31 %	380±35	12.52±1.3 %	0.89
VLPs	6922±726	1316±70	19.0±1.04 %	1033±38	15.09±1.14 %	1.27
PBS	1328±29	453±18	34.0±1 %	229±10	18.78±0.35 %	1.98

purification, and fusion protein detection. SUMO protein has a specific structure comprising a hydrophilic group in the outer layer and a hydrophobic group in the inner layer; this structure allows SUMO protein to function as emulsifiers to interfere with inclusion body formation effectively, thereby improving solubility (Malakhov et al. 2004). In addition, SUMO protease can recognize the tertiary structure of the SUMO-fusion tag, which can produce accurate N-terminal amino acids of fusion proteins and avoid producing extraneous residues at the N terminus of a target protein (Butt et al. 2005).

A high molecular weight and a weak hydrophilic property of CPV VP2 protein, predicted by ExPASy web server, are two characteristics that enable this protein to aggregate easily in inclusion bodies. To induce CPV VP2 protein soluble expression and ensure a highly efficient assembly of VLPs, we constructed a SUMO-VP2 fusion expression system. We also performed this procedure to produce a soluble and high-yield CPV VP2 protein in *E. coli*, which causes the CPV VP2 protein to fuse with SUMO tag, maintaining natural activities. The results further confirmed that SUMO tag can improve the solubility of target proteins, particularly proteins with high molecular weight and weak hydrophilicity.

Protein folding can be affected by many factors, such as temperature, pH, ionic strength, dissolution process, and small molecules with bioactivity (Delos et al. 1995; Yin et al. 2010; Zhao et al. 1995). Although the appropriate temperature to package a CPV virion in a natural host is 37°C, the folding temperature of VLPs in this study was maintained at 4°C to avoid undesirable aggregation and other chemical degradation of the target protein. The results showed that the efficiency of CPV VLP assembly was promoted at 4°C (data not shown).In addition, the assembly of CPV VLPs can be affected by intermolecular interactions. In general, non-polar residues in the inner layer of proteins cannot interact with water molecules to form hydrogen bonds; instead, proteins tend to interact via hydrophobic interactions. Thus, at high salt concentrations or high temperatures, hydrophobic interactions increase and result in protein aggregation (Marshak et al. 1996).This finding can explain why the size of CPV VLPs increased as temperature or salt concentration increased in DLS. The physicochemical property of VP2 was also indicated.

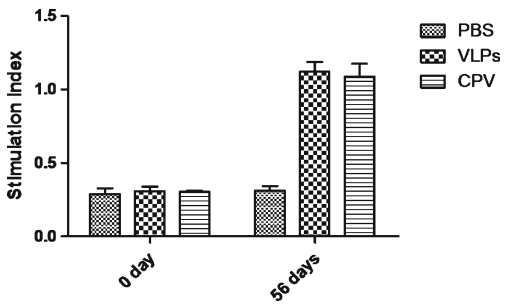

Fig. 6 Lymphoid proliferation assay of mice

Although we cannot confirm the exact assembly efficiency of VLPs under the optimal condition (pH 7.0 and 150 mM NaCl), it was estimated that the assembly efficiency of VLPs is optimal or totally. Hence, the quantity of inoculation was showed as total proteins purified. ELISA test showed that CPV VLPs can induce effective and specific CPV antibodies, particularly neutralization antibodies. The titers of CPV antibody and neutralization antibody did not exhibit significant differences with those of mice immunized with a CPV virion. CPV VP2 proteins expressed in *E. coli* exhibits a natural bioactivity; this result also suggested that the antigen epitopes of CPV VP2 accurately resemble a natural CPV virion, which is consistent with the structure of CPV VP2 by ExPASy software analysis. The results further confirmed that the CPV VLPs correctly assemble. A previous study indicated that neutralizing antibodies bind to either the region common to A site antibodies or the region common to B site antibodies, suggesting that these regions have a unique property (Hafenstein et al. 2009). Hence, the correct presentation of these sites on a viral capsid ensures an effective immune response, particularly specific antibody and neutralization antibody response. This result is also confirmed in this study regarding specific antibody and neutralization antibody titer.

The percentage and ratio of CD4+ and CD8+ T-lymphocytes are the key parameters of immune system (Dhur et al. 1991). CD4+ T-cells differentiate into two phenotypes: T-helper type 1 (Th1) cells, which stimulate immune responses to a cell-mediated immune signal, and T-helper type 2 (Th2) cells, which promote humoral or allergic responses (Constant and Bottomly 1997). CD8+ T-cells can induce the death of infectedsomatic or tumor cells; these T-cells kill virally infected cells (or other cells infected with other pathogens). CD8+ T-cells also eradicate damaged or dysfunctional cells. The present study demonstrated that CPV and CPV VLPs can elicit T-lymphocyte proliferative responses and change the CD4+/CD8+ ratio after immunization. Although

the response of T-lymphocyte proliferation in mice immunized with CPV was higher than that in mice immunized with CPV VLPs, the percentage of CD4+ or CD8+ T-cells in mice immunized with CPV VLPs was higher than that in mice immunized with CPV virion. This result suggested that CPV VLPs could induce a more effective cell-medicated immune response against CPV infections compared with CPV virion.

In conclusion, CPV VP2 proteins expressed in prokaryotic systems can assemble to form VLPs in vitro; however, the mechanism has not been demonstrated yet. After the SUMO tag was introduced to VP2 protein, VP2 protein was expressed with high solubility and can assemble to form VLPs under appropriate conditions. The CPV VLPs exhibiting a natural structure could stimulate specific humoral and cellular immune responses against CPV. CPV VLPs could be a new vaccine candidate of CPV with high yield, safety, and efficiency.

Acknowledgements This research was supported in part by grants from the Fundamental Research Funds for the Chinese Academy of Agricultural Sciences (2013ZL035), Gansu Provincial Sci. & Tech. Department (No. 1102NKDA033; No.1102NKDA034; No.1104WCGA185), National Natural Science Foundation of China (No. 31100688; No. 31101838) and the Scientific Research Foundation for the Returned Overseas Chinese Scholars, State Education Ministry.

References

Arnold K, Bordoli L, Kopp J, Schwede T (2006) The SWISS-MODEL workspace: a web-based environment for protein structure homology modelling. Bioinformatics 22(2):195–201. doi:10.1093/bioinformatics/bti770

Butt TR, Edavettal SC, Hall JP, Mattern MR (2005) SUMO fusion technology for difficult-to-express proteins. Protein Expr Purif 43(1):1–9. doi:10.1016/j.pep.2005.03.016

Chang CF, Wang M, Ou WC, Chen PL, Shen CH, Lin PY, Fang CY, Chang D (2011) Human JC virus-like particles as a gene delivery vector. Expert Opin Biol Ther 11(9):1169–1175. doi:10.1517/14712598.2011.583914

Constant SL, Bottomly K (1997) Induction of Th1 and Th2 CD4+ T cell responses: the alternative approaches. Annu Rev Immunol 15:297–322. doi:10.1146/annurev.immunol.15.1.297

Dahiya SS, Saini M, Kumar P, Gupta PK (2012) Immunogenicity of a DNA-launched replicon-based canine parvovirus DNA vaccine expressing VP2 antigen in dogs. Res Vet Sci 93(2):1089–1097. doi:10.1016/j.rvsc.2012.01.017

Delos SE, Cripe TP, Leavitt AD, Greisman H, Garcea RL (1995) Expression of the polyomavirus minor capsid proteins VP2 and VP3 in *Escherichia coli*: in vitro interactions with recombinant VP1 capsomeres. J Virol 69(12):7734–7742

Dhur A, Galan P, Preziosi P, Hercberg S (1991) Lymphocyte subpopulations in the thymus, lymph nodes and spleen of iron-deficient and rehabilitated mice. J Nutr 121(9):1418–1424

Gallo Calderon M, Wilda M, Boado L, Keller L, Malirat V, Iglesias M, Mattion N, La Torre J (2012) Study of canine parvovirus evolution: comparative analysis of full-length VP2 gene sequences from *Argentina* and international field strains. Virus Genes 44(1):32–39. doi:10.1007/s11262-011-0659-8

Grgacic EV, Anderson DA (2006) Virus-like particles: passport to immune recognition. Methods 40(1):60–65. doi:10.1016/j.ymeth.2006.07.018

Guex N, Peitsch MC (1997) SWISS-MODEL and the Swiss-PdbViewer: an environment for comparative protein modeling. Electrophoresis 18(15):2714–2723. doi:10.1002/elps.1150181505

Guo HC, Sun SQ, Jin Y, Yang SL, Wei YQ, Sun DH, Yin SH, Ma JW, Liu ZX, Guo JH, Luo JX, Yin H, Liu XT, Liu DX (2013) Foot-and-mouth disease virus-like particles produced by a SUMO fusion protein system in *Escherichia coli* induce potent protective immune responses in guinea pigs, swine and cattle. Vet Res 44:48. doi:10.1186/1297-9716-44-48

Hafenstein S, Bowman VD, Sun T, Nelson CD, Palermo LM, Chipman PR, Battisti AJ, Parrish CR, Rossmann MG (2009) Structural comparison of different antibodies interacting with parvovirus capsids. J Virol 83(11):5556–5566. doi:10.1128/JVI.02532-08

Ionescu RM, Przysiecki CT, Liang X, Garsky VM, Fan J, Wang B, Troutman R, Rippeon Y, Flanagan E, Shiver J, Shi L (2006) Pharmaceutical and immunological evaluation of human papillomavirus viruslike particle as an antigen carrier. J Pharm Sci 95(1):70–79. doi:10.1002/jps.20493

Johnson JE, Chiu W (2000) Structures of virus and virus-like particles. Curr Opin Struct Biol 10(2):229–235. doi:10.1016/S0959-440X(00)00073-7

Kitai Y, Fukuda H, Enomoto T, Asakawa Y, Suzuki T, Inouye S, Handa H (2011) Cell selective targeting of a simian virus 40 virus-like particle conjugated to epidermal growth factor. J Biotechnol 155(2):251–256. doi:10.1016/j.jbiotec.2011.06.030

Langeveld JP, Casal JI, Vela C, Dalsgaard K, Smale SH, Puijk WC, Meloen RH (1993) B-cell epitopes of canine parvovirus: distribution on the primary structure and exposure on the viral surface. J Virol 67(2):765–772

Malakhov MP, Mattern MR, Malakhova OA, Drinker M, Weeks SD, Butt TR (2004) SUMO fusions and SUMO-specific protease for efficient expression and purification of proteins. J Struct Funct Genomics 5(1–2):75–86. doi:10.1023/B:JSFG.0000029237.70316.52

Marshak DR, Kadonaga JT, Burgess RR, Knuth MWJWAB, Lin S-H (1996) Strategies for protein purification and characterization. A laboratory course manual. Cold Spring Harbor Laboratory Press, New York, xviii + 396p

Mihailova M, Boos M, Petrovskis I, Ose V, Skrastina D, Fiedler M, Sominskaya I, Ross S, Pumpens P, Roggendorf M, Viazov S (2006) Recombinant virus-like particles as a carrier of B- and T-cell epitopes of hepatitis C virus (HCV). Vaccine 24(20):4369–4377. doi:10.1016/j.vaccine.2006.02.051

Mohan RJ, Mukhopadhyay HK, Thanislass J, Antony PX, Pillai RM (2010) Isolation, molecular characterization and phylogenetic analysis of canine parvovirus. Infect Genet Evol 10(8):1237–1241. doi:10.1016/j.meegid.2010.08.005

Ntafis V, Mari V, Decaro N, Papanastassopoulou M, Papaioannou N, Mpatziou R, Buonavoglia C, Xylouri E (2011) Isolation, tissue distribution and molecular characterization of two recombinant canine coronavirus strains. Vet Microbiol 151(3–4):238–244. doi:10.1016/j.vetmic.2011.03.008

Park JS, Choi BK, Vijayachandran LS, Ayyappan V, Chong CK, Lee KS, Kim SC, Choi CW (2007) Immunodetection of Canine Parvovirus (CPV) in clinical samples by polyclonal antisera against CPV-VP2 protein expressed in *Esherichia coli* as an antigen. J Virol Methods 146(1–2):281–287. doi:10.1016/j.jviromet.2007.07.021

Parrish CR (1990) Emergence, natural history, and variation of canine, mink, and feline parvoviruses. Adv Virus Res 38:403–450

Parrish CR, Aquadro CF, Strassheim ML, Evermann JF, Sgro JY, Mohammed HO (1991) Rapid antigenic-type replacement and DNA sequence evolution of canine parvovirus. J Virol 65(12):6544–6552

Patial S, Chaturvedi VK, Rai A, Saini M, Chandra R, Saini Y, Gupta PK (2007) Virus neutralizing antibody response in mice and dogs with a bicistronic DNA vaccine encoding rabies virus glycoprotein and canine parvovirus VP2. Vaccine 25(20):4020–4028. doi:10.1016/j.vaccine.2007.02.051

Pillay S, Meyers A, Williamson AL, Rybicki EP (2009) Optimization of chimeric HIV-1 virus-like particle production in a baculovirus-insect cell expression system. Biotechnol Prog 25(4):1153–1160. doi:10.1002/btpr.187

Sedlik C, Sarraseca J, Rueda P, Leclerc C, Casal I (1995) Immunogenicity of poliovirus B and T cell epitopes presented by hybrid porcine parvovirus particles. J Gen Virol 76(Pt 9):2361–2368. doi:10.1099/0022-1317-76-9-2361

Singh P, Destito G, Schneemann A, Manchester M (2006) Canine parvovirus-like particles, a novel nanomaterial for tumor targeting. J Nanobiotechnology 4:2. doi:10.1186/1477-3155-4-2

Tsao J, Chapman MS, Agbandje M, Keller W, Smith K, Wu H, Luo M, Smith TJ, Rossmann MG, Compans RW, Parrish CR (1991) The three-dimensional structure of canine parvovirus and its functional implications. Science 251(5000):1456–1464

Xu J, Guo HC, Wei YQ, Shu L, Wang J, Li JS, Cao SZ, Sun SQ (2013) Phylogenetic analysis of canine parvovirus isolates from Sichuan and Gansu Provinces of China in 2011. Transbound Emerg Dis. doi:10.1111/tbed.12078

Yin S, Sun S, Yang S, Shang Y, Cai X, Liu X (2010) Self-assembly of virus-like particles of porcine circovirus type 2 capsid protein expressed from *Escherichia coli.* Virol J 7:166. doi:10.1186/1743-422X-7-166

Yuan W, Parrish CR (2001) Canine parvovirus capsid assembly and differences in mammalian and insect cells. Virology 279(2):546–557. doi:10.1006/viro.2000.0734

Zhao X, Fox JM, Olson NH, Baker TS, Young MJ (1995) In vitro assembly of cowpea chlorotic mottle virus from coat protein expressed in *Escherichia coli* and in vitro-transcribed viral cDNA. Virology 207(2):486–494. doi:10.1006/viro.1995.1108